IS-T-578

MASTER

GROWTH OF SINGLE CRYSTALS OF HEXAGONAL NICKEL SULFIDE

M.S. Thesis Submitted to Iowa State University,
February, 1973

F. D. Trumpy

Ames Laboratory, USAEC
Iowa State University
Ames, Iowa 50010

Date of Manuscript: February, 1973

PREPARED FOR THE U. S. ATOMIC ENERGY COMMISSION
DIVISION OF RESEARCH UNDER CONTRACT NO. W-7405-eng-82

DISCLAIMER

Available from: National Technical Information Service
Department A
Springfield, VA 22151

Price: Microfiche $0.95

Growth of single crystals of hexagonal nickel sulfide

by

Franklin Dale Trumpy

A Thesis Submitted to the

Graduate Faculty in Partial Fulfillment of

The Requirements for the Degree of

MASTER OF SCIENCE

Department: Physics
Major Subject: Solid State Physics

Approved:

G. C. Danielson
In Charge of Major Work

For the Major Department

For the Graduate College

Iowa State University
Ames, Iowa

1972

TABLE OF CONTENTS

LIST OF TABLES

LIST OF FIGURES

ABSTRACT

Single crystals have been grown of hexagonal nickel sulfide of varying stoichiometry. The Bridgman method was used to produce large ingots 1.3 cm in diameter and 3-4 cm long. The lattice parameters and nickel to sulfur ratios have been determined for samples cut from these ingots. The resistivity of five samples have been measured from 4.2 to 300 K by a four-probe technique. The data indicated that a metal-to-semiconductor transition did not occur in hexagonal Ni_xS samples when $x \geq 1.02$, but did suggest that the magnetic transition persisted. For sulfur-rich samples with $x = 0.996$, the metal-to-semiconductor transition was observed. Resistivity measurements on oriented single crystals showed an anisotropy in the electrical conductivity. The electrical resistance in the basal plane was about twice the resistance perpendicular to the basal plane at 4.2 K.

I. INTRODUCTION

Systems which display abrupt changes in their physical properties as a function of some external variable capture the interest of scientists. Gradual changes in physical properties are intuitively more comprehensible and less interesting than the sudden transition. For example, a material that displays a metal-semiconductor transition in its electrical conductivity is more intriguing than either the metal or the semiconductor. Likewise, a material displaying a para-antiferromagnetic transition generates more interest and curiosity than either the paramagnet or the antiferromagnet.

Hexagonal nickel sulfide is doubly intriguing in that it possess both a metal-semiconductor and a para-antiferromagnetic transition simultaneously as a function of temperatures. The magnetic transition in hexagonal NiS was reported by Sparks and Komoto in 1963.[1] The electrical transition was also reported by Sparks and Komoto four years later in 1967.[2] In both cases, powdered samples of hexagonal NiS were measured and the simultaneous transitions occurred at 264 ± 1 K.

Subsequent neutron diffraction studies by Smith, Sparks, and Komoto[3,4] have been performed. These studies showed an abrupt increase in the a and c lattice parameters of 0.33% and 1% respectively upon cooling through 263 K. In addition, they also showed that below T_N the nickel moments of approximately $1.7\ \mu_B$ are coupled ferromagnetically in the basal planes and adjacent basal planes are coupled antiferromagnetically.

Sparks and Komoto have also studied nonstoichiometric NiS and have predicted no transition for $x \lesssim 0.96$.[5]

A theory of semiconductor-to-metal transitions has been proposed by Adler and Brooks[6] in which they suggest that a metal-to-semiconductor transition may arise from an antiferromagnetic exchange interaction. Hexagonal NiS is the only known material which has an electrical transition that may be due to an antiferromagnetic interaction.

The present investigation is concerned with growth, preparation, and measurement of single crystals of hexagonal nickel sulfide of varying stoichiometry. A method is presented for the growth of large single crystals of hexagonal nickel sulfide. Results on the x-values of some nickel sulfide samples, their lattice parameters, and electrical and magnetic properties are discussed.

II. THE STRUCTURE OF NICKEL SULFIDE

Stoichiometric nickel sulfude can exist in two different structures. At temperatures below 620 K, stoichiometric nickel sulfide forms a rhombohedral structure called millerite. The millerite phase of nickel sulfide is known to be metallic in electrical character from 1100 to 300 K.[7] At temperatures above 620 K, NiS forms a hexagonal NiAs-type structure whose lattice parameters are a = 3.4392 Å and c = 5.3484 Å.[8]

Figure 1 shows the NiAs-type structure for nickel sulfide. In Fig. 1, the open circles represent nickel atoms and the solid dots represent sulfur atoms. The arrows on the open circles illustrate the magnetic structure below the para-to-antiferromagnetic transition temperature according to Sparks and Komoto.[1]

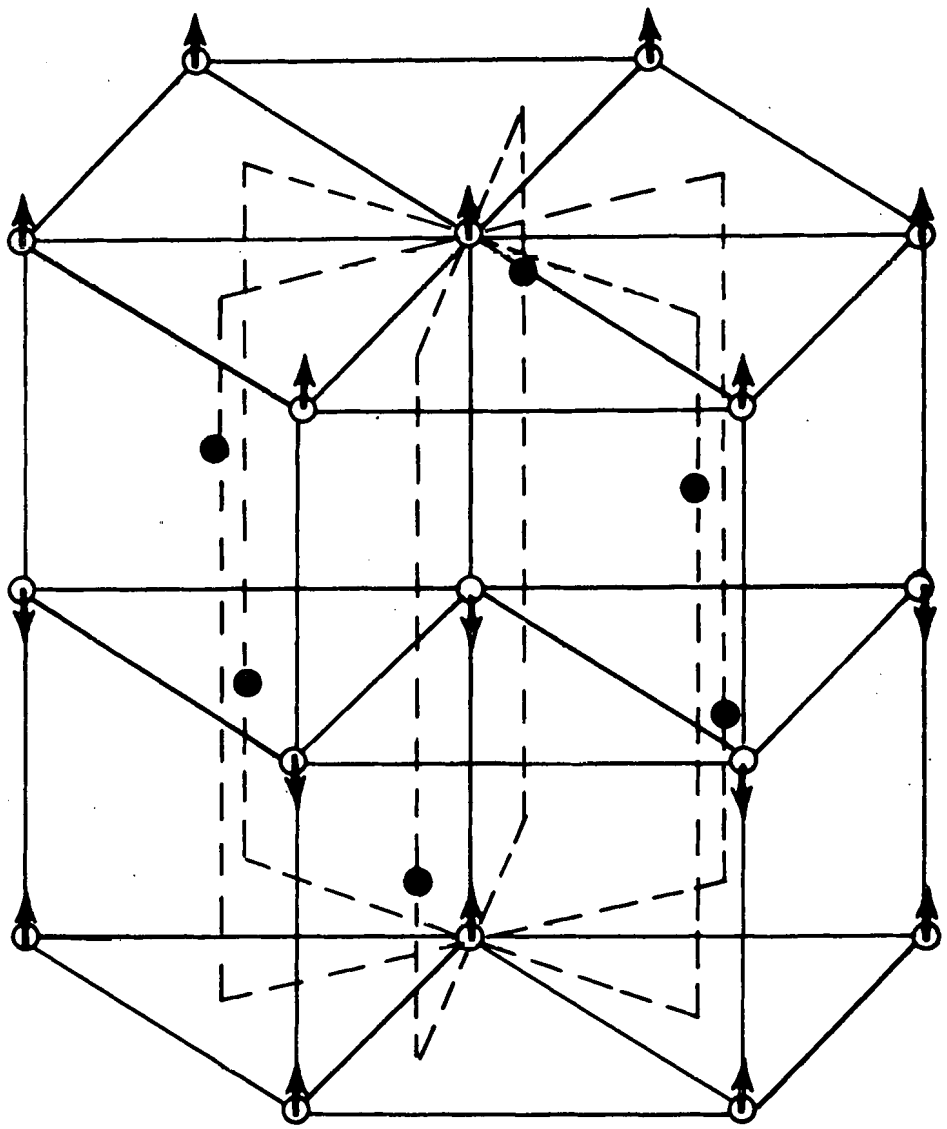

Fig. 1. The NiAs-type structure of nickel sulfide showing the positions of the nickel and sulfur atoms. The arrows indicate the magnetic structure below the transition temperature

III. GROWTH OF SINGLE CRYSTALS OF HEXAGONAL NICKEL SULFIDE

In this investigation the Bridgman technique was used to grow single crystals of hexagonal NiS. In this method, a bomb containing the materials to be reacted is placed in a vertically shafted furnace having a negative temperature gradient from top to bottom. The bomb is lowered into the furnace from the top where a temperature is maintained that is sufficient to allow reaction and melting. After an adequate period of time for reaction and melting, the bomb is slowly lowered through the furnace and passes through the solidification temperature of the compound. At this time, the solidifying compound grows as a single crystal from bottom to top.

The chemicals used in the earliest Bridgman furnace runs of this investigation were Baker Analyzed Reagent nickel from the J. T. Baker Chemical Company and Sulfur, N. F. (sublimed) manufactured by Fisher Scientific Company. Later crystals were grown with 99.995% pure nickel powder from Electronic Space Products, Inc. and 99.999+% pure sulfur from the American Smelting and Refining Company.

The materials were weighed out in proportions to produce the desired stiochiometry. The sulfur was first loaded into the fused quartz Bridgman crucible illustrated in Fig. 2a. Next, the nickel powder was loaded in the crucible on top of the sulfur. It is important to load the materials in this order to avoid sulfur being heated and pumped away when the crucible is sealed. The crucible was then slowly pumped on until a pressure of 30 to 40 microns was achieved and then the crucible was sealed. It was important to pump down the

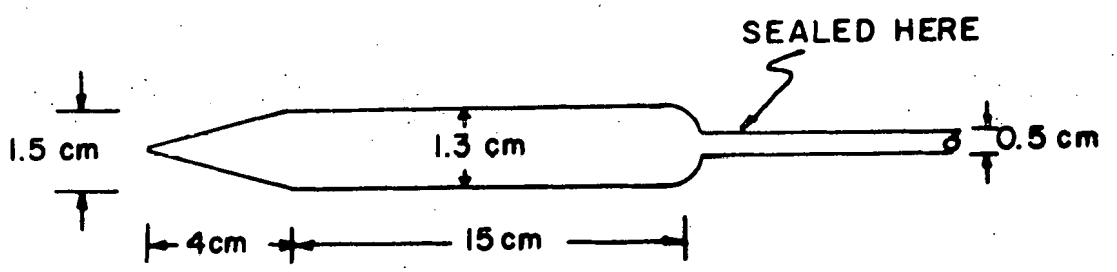

Fig. 2a. Fused quartz Bridgman crucible

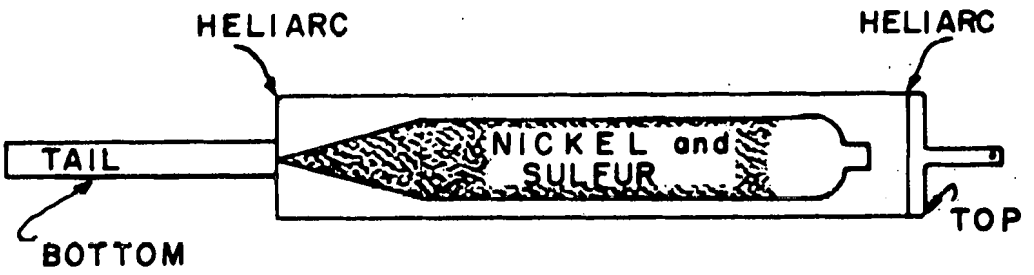

Fig. 2b. Stainless steel Bridgman bomb with crucible sealed inside

crucible slowly to avoid pumping nickel powder into the cold trap. Once the quartz Bridgman crucible was sealed, it was placed inside a stainless steel bomb as illustrated in Fig. 2b and the bomb was sealed by the heliarc process.

The sealed unit of bomb and crucible was suspended by the lowering cable so that the lowest point on the bomb was at least five centimeters above the upper opening to the Bridgman furnace. The lowering process was begun at this point with a lowering speed of 1.0 cm/hr. This step assured that the sulfur would not heat up too rapidly and rupture the quartz crucible. Once the bomb was entirely inside the furnace, the lowering speed was reduced to 0.5 cm/hr - 1.0 cm/hr. Time for traversing the entire length of the furnace was approximately five days to one week for most runs.

Since hexagonal nickel sulfide is the high temperature nickel sulfide structure, it was necessary to quench in the hexagonal structure. The hexagonal structure being present above 620 K, all ingots were quenched from 425 $\pm$ 25 C to air at room temperature or to water and ice at 0 C.

Table 1 shows the results of several Bridgman runs and the conditions under which the crystals were grown. Run number 7 in Table 1 shows the importance of a sufficiently high temperature to insure a complete melt. A minimum temperature of 900 C was necessary to assure adequate melting of the materials. Run numbers 11 and 12 were run under nearly identical conditions except for lowering speed and quenching procedure. Run number 11 resulted in a crystal of mixed

Table 1. Growth conditions for some nickel sulfide runs

Run Number	Furnace Temperatures Top	Middle	Bottom	Lowering Speed	Time in Furnace	Quench	Results
7	600 C	450 C	200 C	1.0 cm/hr	94 hrs	ice	Incomplete melting
8	900 C	690 C	450 C	lowered manually	120 hrs	water & ice	Single crystal
11	980 C	790 C	490 C	0.75 cm/hr	144 hrs	water	Single crystal mixed phase
12	980 C	790 C	490 C	0.5 cm/hr	150 hrs	water & ice	Several large grains of single crystal
17	911 C	677 C	470 C	0.5 cm/hr	288 hrs	water & ice	Single crystal
20	910 C	581 C	360 C	0.5 cm/hr	240 hrs	water & ice	Two grains of single crystal and amorphous material
21	962 C	650 C	415 C	1.0 cm/hr	96 hrs	water & ice	Polycrystalline ingot and some amorphous material

phase (both high and low temperature phases present) while run number 12 resulted in a crystal of purely hexagonal nickel sulfide. Experience with run number 8, which was lowered manually at approximately 100 cm/hr, indicated the relative insensitivity of structure formed to the lowering speed. Therefore, it was concluded that the quench in water and ice at 0 C aided in quenching in the hexagonal structure. All subsequent runs were quenched in water and ice. Table 1 indicates that the crucial factors in the growth of hexagonal nickel sulfide are temperature and quenching techniques.

The method presented here for the growing of hexagonal nickel sulfide has proved to be about 50% successful. Failure of the technique was usually due to one of two factors. By far, the greatest problem was the rupturing of quartz crucibles. Crucible ruptures usually occurred when the bomb was first introduced into the furnace. The crucible occasionally ruptured upon quenching but this was not a serious problem since the crystal ingot was already formed. The second and equally serious cause of failure was due to incomplete quenching. Incomplete quenching resulted in ingots where both the high and low temperature structures existed simultaneously. Attempts to cycle out the low temperature phase in an annealing furnace were unsuccessful.

IV. PREPARATION AND ANALYSIS OF SAMPLES

Samples were prepared from ingots grown by the method described in Section III. The cutting of samples was achieved by both a spark cutter and a wire-saw using silicon carbide as a cutting compound. However, the wire-saw was found to be most satisfactory from the standpoint of minimum crystal damage. The spark cutter tended to pit the crystals and leave very uneven edges. All samples were shaped as parallelopipeds with a minimum length of width ratio of 4 to 1 to minimize end effects.

Since spring loaded tungsten probes, as described in Section V, were used to measure sample resistivity, two pits were placed in each sample to provide a secure resting place for the tungsten probes. Pitting was achieved by masking each sample with cellophane tape in which two small holes were placed by a very sharp steel probe. The masked samples were then lightly sprayed with an air-brasive tool to form the pits.

Most samples were cut randomly with respect to orientation to the symmetry axes of the crystals. Samples cut with definite orientations were oriented using Laue diffraction patterns. Crystal structure and lattice parameters were determined by Debye-Scherrer x-ray analysis. Chemical analysis was used to determine x-values of all NiS samples.

V. ELECTRICAL MEASUREMENTS

The apparatus used to measure resistivity is shown by block diagram in Fig. 3. Voltages were measured using a Leeds-Northrop K-3 Universal Potentiometer and a Leeds-Northrop Model 9834 null detector. Current was supplied to the sample with a Power Designs Model 5055R regulated d.c. power supply. The current flowing through the sample was determined by measuring the voltage drop across a one milliohm standard resistor. Temperature control was achieved using a d.c. power supply constructed by Louis D. Muhlestein.[9]

All measurements were made using the four probe technique illustrated in Fig. 4. The voltage probes consisted of 0.010 inch tungsten wire sharpened by dipping in boiling sodium nitrite. The tungsten probes were spring loaded with phosphor bronze springs. Current to the sample was supplied through spring loaded, indium padded copper blocks. A small diamond chip was placed between the sample and the copper base of the holder to assure good thermal contact with adjacent thermometers.

Temperatures were measured with copper-constantan and gold (0.03% iron)-copper thermocouples referred to a 273.18 K ice bath.

The electrical resistivity of samples in this investigation were determined by

$$\rho = \frac{V}{I}\frac{A}{L} \quad ,$$

where ρ is the resistivity, V is the voltage measured between the

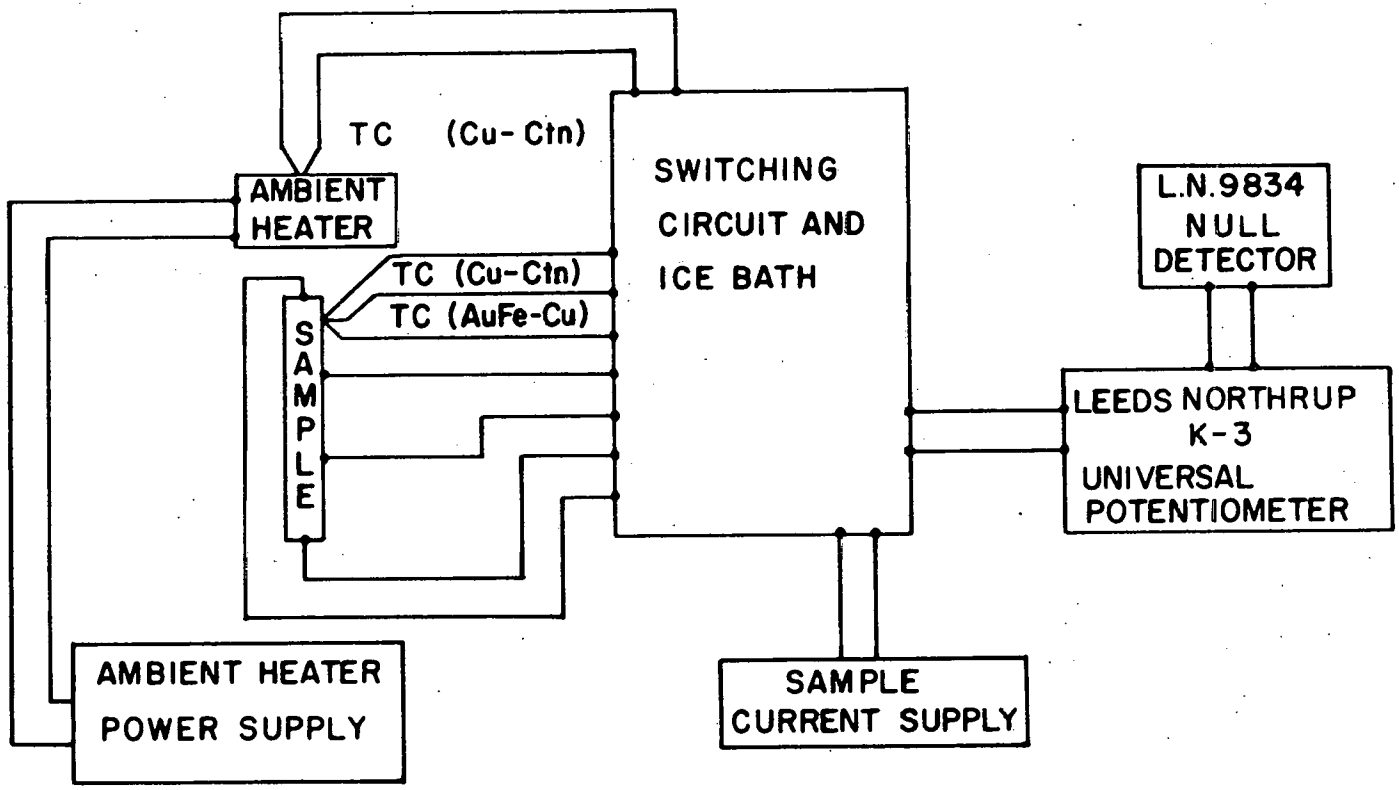

Fig. 3. A block diagram of the electrical resistivity apparatus

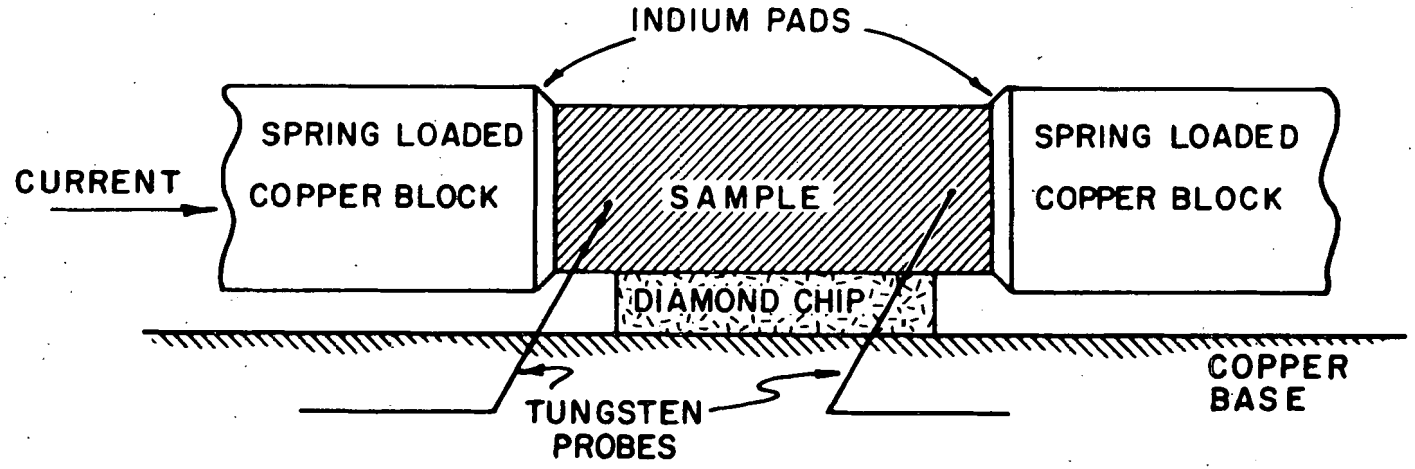

Fig. 4. Sample holder used in the four-probe technique. The current blocks and voltage probes were loaded with helical phosphor bronze springs

probes, I is the current flowing through the sample, A is the cross-sectional area of the sample, and L is the distance between probes. If the voltage is measured in microvolts, the current in amperes, and A/L in centimeters, then the resistivity is expressed in micro-ohm-centimeters ($\mu\Omega$-cm). Measurements were taken with the current in both directions and averaged to eliminate thermoelectric effects.

Figure 5 shows a plot of the resistivity versus temperature for sample 8-h. Sample 8-h is $Ni_{0.996}S$. An abrupt increase in the resistivity is observed at approximately 200 K. For the same stoichiometry, using compressed, powdered sample data, Sparks and Komoto predict a transition temperature of 250 K. More confidence was placed in the 200 K transition temperature. Resistivity measurements on single crystals are more reliable than those made on powdered samples. For comparison, Fig. 5 also shows data taken on a compressed powder by Sparks and Komoto. This data has been adjusted so that the resistivity at 0 C is 1 $\mu\Omega$-cm. Sparks and Komoto's sample differs from that of the present investigation in two aspects. The powdered sample displays a larger change in resistivity than the single crystals of this investigation. It is not clear why the discrepancy occurs, but may be due to the differing stoichiometries of the two materials.

The structure of the curves below the transition temperature also differ. Fig. 6 shows a plot of $\log \rho$ versus $10^3/T$ for both samples below the transition temperature. The resistivity of Sparks and Komoto's data has been scaled so that $\rho(0\ C) = 0.5\ \mu\Omega$-cm for purposes of illustration. While the resistivity of sample 8-h tends to drop

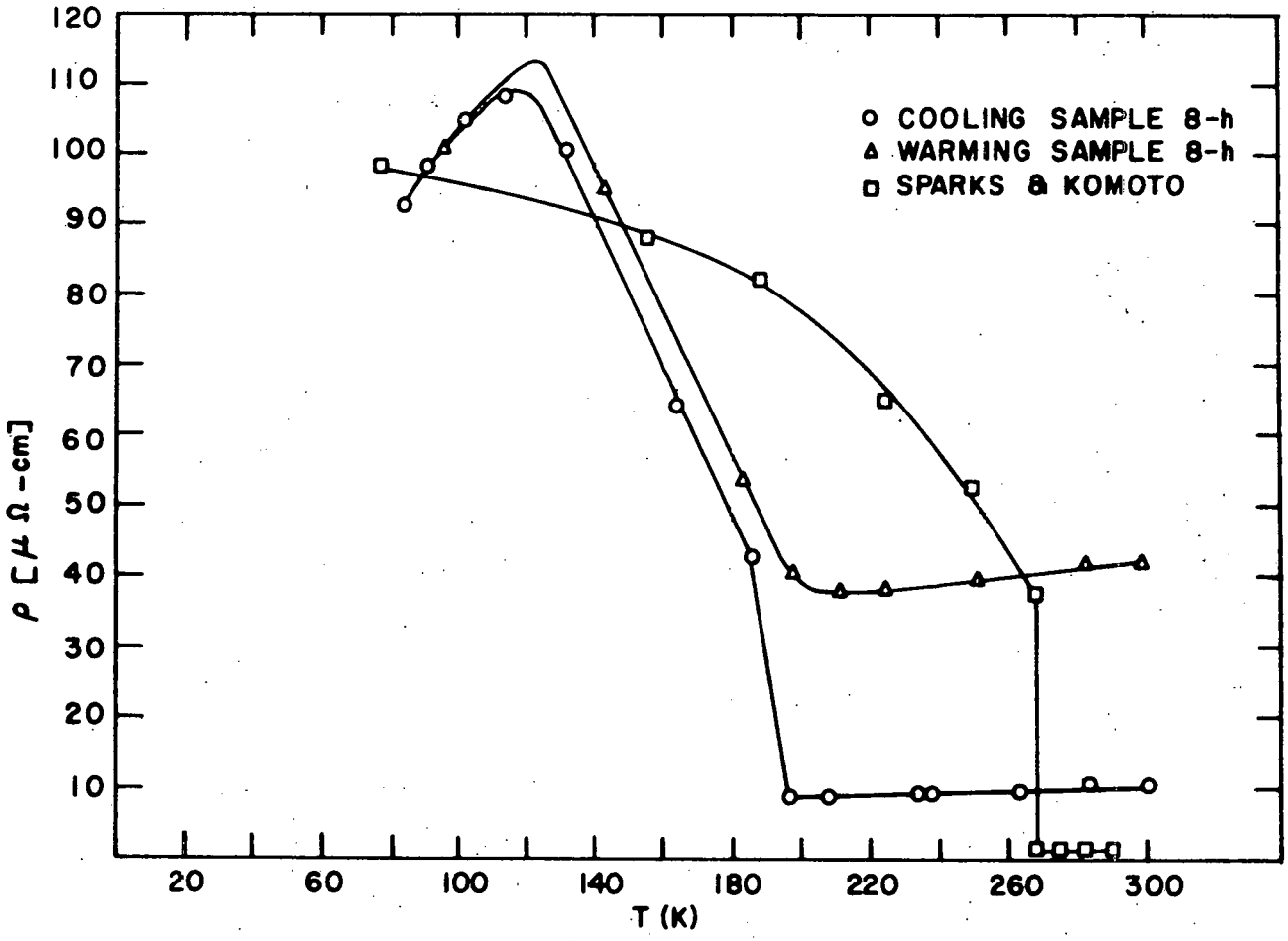

Fig. 5. A plot of electrical resistivity versus temperature for sample 8-h ($\dot{x}$ = 0.996) showing an electrical transition. Data taken on a powdered sample by Sparks and Komoto is shown for comparison

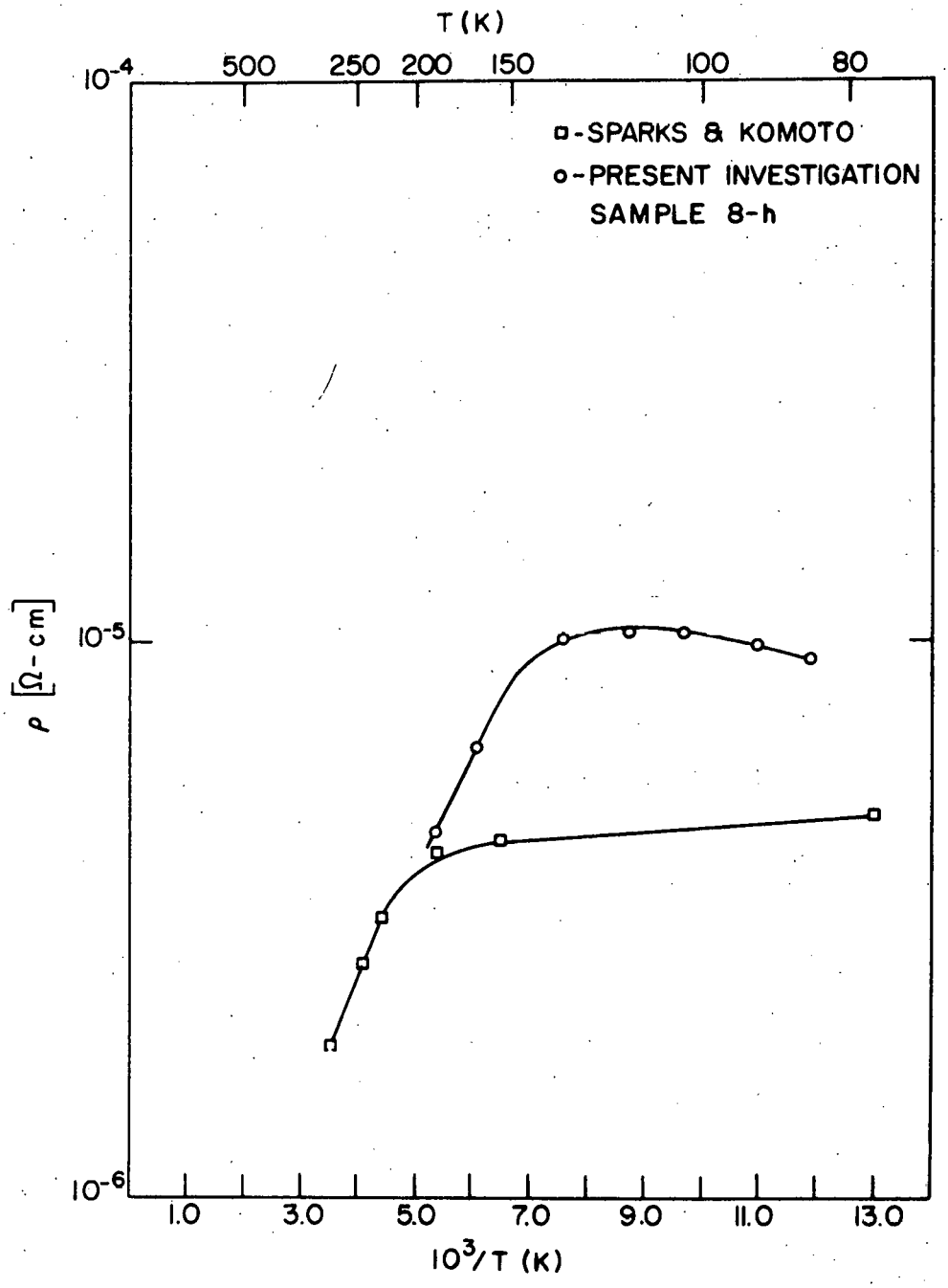

Fig. 6. A plot of $\log \rho$ versus $10^3/T$ for sample 8-h in the region below the transition temperature. Sparks and Komoto's data has been included for comparison

with lowering temperature, the resistivity of Sparks and Komoto's material tends to rise slightly. Different impurities in the two materials may account for this difference. In the region 186 - 160 K the activation energy for conduction in sample 8-h was calculated to be 0.12 eV, in excellent agreement with Sparks and Komoto.[2]

Figure 5 also shows a severe hystersis in the warming curve of the single crystal sample. Inspection of samples that had passed through the transition temperature indicated extensive cracking. The hystersis, therefore, has been attributed to sample cracking. Sample cracking upon passing through the transition temperature occurred only for those samples possessing an electrical transition.

Figure 7 shows a plot of resistivity versus temperature for samples 12-c, 12-d, 12-g, and 17-a. The x-values for these and other samples are listed in Table 2. No electrical transition was observed in these nickel-rich samples. However, a change in slope of the resistivity curve was observed in the neighborhood of 200 K.

Results of the electrical measurements on nickel-rich hexagonal nickel sulfide suggest that nonstoichiometric Ni_xS where $x \gtrsim 1.018$ may not display an electrical transition. The structure of the plots for these samples is very similar to those of other materials undergoing magnetic transitions.[10] Therefore, a possible explanation for the change in slope is that a para-to-antiferromagnetic transition occurred while the electrical transition was suppressed. Figure 7 also shows an apparent anisotropy in the electrical conductivity. The electrical resistivity in the basal plane was about twice the resistivity perpendicular to the basal plane at 4.2 K.

Table 2. The physical parameters and orientations of some hexagonal NiS samples

Sample	Lattice Parameters		X-Value	Orientation	Electrical Transition?
	a	c			
8-h	3.4239 ± .0016 Å	5.3280 ± .0015 Å	0.996	Random	Yes
8-c	3.4239 ± .0012 Å	5.3276 ± .0011 Å	0.995	Random	Yes
12-c	3.4241 ± .0035 Å	5.3119 ± .0033 Å	1.02	I∥C	No
12-d	3.4241 ± .0035 Å	5.3119 ± .0033 Å	1.02	Random	No
12-g	3.4241 ± .0035 Å	5.3119 ± .0033 Å	1.02	I⊥C	No
17-a	3.4217 ± .0011 Å	5.3137 ± .0008 Å	1.018	I⊥C	No

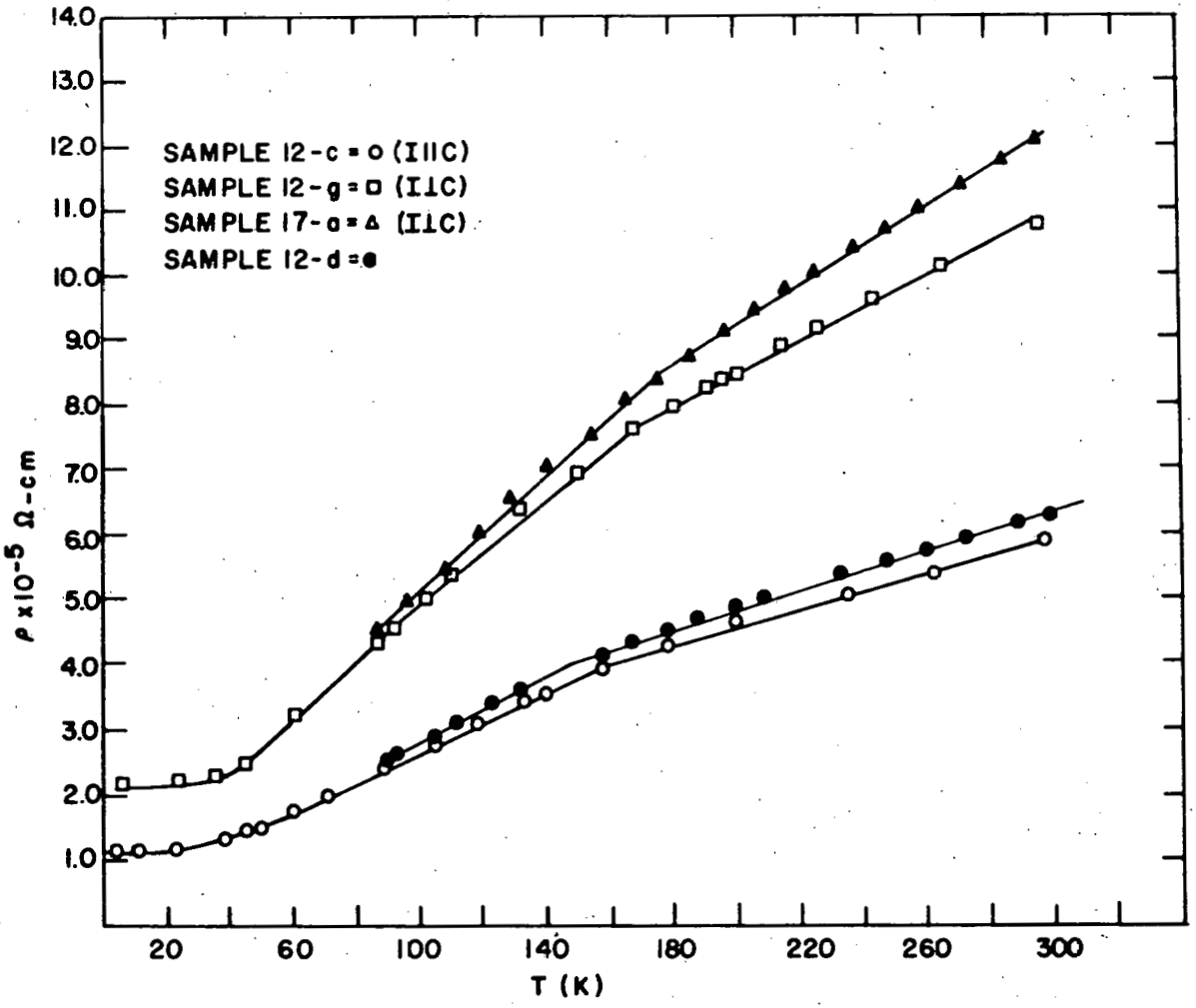

Fig. 7. A plot of electrical resistivity versus temperature for various nickel-rich samples in which no electrical transition was observed

VI. SUMMARY

Single crystals of hexagonal nickel sulfide have been grown with varying stoichiometry. The most significant factors in using the Bridgman method to grow hexagonal NiS have been found to be furnace temperature and quenching rate. For successful runs, the minimum temperature at the top of the furnace was 900 C and all bombs were quenched in ice and water. The success rate for this method might be increased by using thicker walled quartz crucibles to prevent rupture. This investigation has led the author to conclude that the Bridgman technique is a suitable method for growing hexagonal NiS.

The resistivity measurements made in this investigation had some unexpected results. The electrical transition appears to be suppressed in samples sufficiently nickel-rich. For the samples measured in this investigation, no electrical transition was observed for $x \geq 1.018$. The structure of the resistivity versus temperature curves for these samples, however, suggest that a magnetic transition is occurring. Preliminary magnetic measurements have indicated that these nickel-rich samples do undergo a magnetic transition and that the transition is antiferromagnetic in nature. Presently, the data on this subject is not complete enough to be conclusive. In addition, the nickel-rich samples displayed an anisotropy in their electrical conductivity. The electrical resistivity in the basal plane was about twice the resistivity perpendicular to the basal plane at 4.2 K.

Electrical resistivity measurements on other samples where $x < 1.000$ revealed an electrical transition. The data for these samples compared favorably with that of Sparks and Komoto. It is especially encouraging that the linear region from 186 - 162 K possessed the same activation energy as powdered samples measured by Sparks and Komoto. This suggests that the linear region is the intrinsic line of semiconducting hexagonal NiS with a 0.24 eV gap energy.

Looking to the future, more electrical measurements are needed on hexagonal NiS. The hall coefficients and mobilities of hexagonal NiS measured as the material passes through the transition temperature will provide insight into the nature of the electrical transition that occurs. Measurements will be made continuously from the metallic to the semiconducting state using an a.c. hall apparatus capable of detecting one nanovolt signals.

VII. LITERATURE CITED

1. J. T. Sparks and T. Komoto, J. Appl. Phys. 34, 1191 (1963).
2. J. T Sparks and T. Komoto, Phys. Letters 25A, 398 (1967).
3. J. T. Sparks and T. Komoto, J. Appl. Phys. 39, 715 (1968).
4. F. A. Smith and J. T. Sparks, J. Appl. Phys. 40, 1332 (1969).
5. J. T. Sparks and T. Komoto, Rev. of Mod. Phys. 40, 752 (1968).
6. D. Adler and H. Brooks, Phys. Rev. 155, 226 (1967).
7. K. Hauffe and H. G. Flindt, Z. Phys. Chem. 200, 199 (1952).
8. M. Laffitte, Bull. Soc. Chim. France (1959), p. 1211-1222.
9. L. D. Muhlestein, Ph.D. Thesis. Ames, Iowa, Library, Iowa State University of Science and Technology (1966).
10. A. L. Trego and A. R. Mackintosh, Phys. Rev. 166, 495 (1968).

VIII. ACKNOWLEDGMENTS

The author wishes to express his appreciation to Dr. Gordon C. Danielson and Mr. Howard R. Shanks for their many helpful discussions and encouragement during this investigation. In addition, the author also wishes to thank Mr. O. M. Sevde for his helpful assistance.